







RESEARCH PAPER

Pharmaceutical prokinetic and surgical interventions have opposing effects on gastroduodenal electromechanical coupling

Sam Simmonds¹  | Tim H.-H. Wang²  | Ashton Matthee¹  | Jarrah M. Dowrick¹  | Andrew J. Taberner^{1,3}  | Peng Du^{1,3}  | Timothy R. Angeli-Gordon^{1,2,4} 

¹Auckland Bioengineering Institute, University of Auckland, Auckland, New Zealand

²Department of Surgery, University of Auckland, Auckland, New Zealand

³Department of Engineering Science and Biomedical Engineering, University of Auckland, Auckland, New Zealand

⁴Te Manawahoukura Rangahau Centre, Te Wānanga o Aotearoa, Te Awamutu, New Zealand

Correspondence

Timothy R. Angeli-Gordon, Auckland Bioengineering Institute, University of Auckland, Auckland, New Zealand.
Email: t.angeli@auckland.ac.nz

Funding information

Royal Society Te Apārangi; Marsden Fund

Abstract

Improper gastric emptying is implicated in several gastrointestinal disorders and may result from disrupted electromechanical coupling of the gastroduodenal junction (GDJ). Rhythmic “slow waves” and myogenic “spikes” are bioelectrical mechanisms that, alongside neural and hormonal co-factors, control GDJ motility.

Aim: To characterize the electromechanical effects of prokinetic (erythromycin) infusion and truncal vagotomy on pre-clinical in vivo porcine models.

Methods: Following ethical approval, the GDJ was exposed in anesthetized crossbreed weaner pigs ($N=10$), and custom high-resolution electrodes were applied to the serosal surface. An EndoFLIP catheter (Medtronic, USA) was inserted orally and positioned across the pylorus to measure luminal diameter. In all subjects, control periods preceded intravenous infusion of erythromycin. In five of those subjects, truncal vagotomy was performed approximately an hour post-infusion, before recording was resumed.

Results: Compared to control recordings, erythromycin increased contractile amplitude ($[2.9 \pm 1.1]$ mm vs. $[2.2 \pm 0.9]$ mm; $p=0.002$) and was associated with more consistent gastric slow-wave rhythms and increased amplitude of slow waves and spikes. Surgical vagotomy immediately decreased contractile amplitude ($[2.90 \pm 1.1]$ mm vs. $[1.2 \pm 0.6]$ mm; $p=0.049$) and was associated with reduced slow-wave amplitude, increased gastric and duodenal slow-wave frequencies, and decreased spike patch coverage.

Conclusions: In conclusion, prokinetics and vagotomy produced opposing effects on GDJ electromechanical coupling and could inform diagnostic and interventional practices for patients with pathophysiological complications of this region.

KEYWORDS

electrophysiology, in vivo experimentation, motility, prokinetics, slow waves, vagotomy

1 | INTRODUCTION

Tonic and phasic contractions across the gastroduodenal junction (GDJ) control gastric emptying,^{1,2} and disruptions in gastric emptying have been associated with gastroparesis,^{3,4} dumping syndrome,⁵ and functional dyspepsia.^{6,7} The pylorus, therefore, remains a critical clinical target, as greater physiological understanding of this region may, in turn, identify a biomarker enabling physicians to characterize patients by pathological cause rather than symptoms.^{8,9}

The motility of gastrointestinal (GI) musculature is controlled by intrinsic bioelectrical, neural, and hormonal factors.¹⁰ Bioelectrical “slow waves” and “spikes” are critical regulatory factors for GI electromechanical coupling that can be readily measured from GI serosa and mucosa using high-resolution electrical mapping techniques.^{11,12} Slow waves have been measured from the antrum and duodenum as phase-locked oscillations in membrane potentials, with each region demonstrating different morphology, frequency, and conductive patterns.^{13,14} In the stomach and duodenum, slow waves are generated by a network of interstitial cells of Cajal (ICC) surrounding the myenteric plexus (ICC-MP), which are coupled to nearby smooth muscle cells (SMC).¹⁵ SMC spike potentials are localized Ca^{2+} transients that are invoked by depolarization¹³ that propagate small distances (i.e., $<50\text{ mm}^2$) in “patches.”^{16,17} Depolarization of GI musculature promotes contraction, and slow waves, therefore, act as a spatiotemporal “scaffold” unto which superimposed spikes may provide further electrical stimulus to modulate force.¹⁸

Impedance planimetry techniques, such as the EndoFLIP (Medtronic, USA), capture GI lumen geometry for immediate visualization and are routinely applied to assess the distensibility of lower esophageal and pyloric sphincters.¹⁹ Pyloric distensibility, GDJ contractility, and gastric emptying^{6,20} are related biomarkers that may indicate a specific diagnosis and appropriate treatment regimen for patients with GI disorders, including gastroparesis^{19,21} and functional dyspepsia.⁷ The clinical efficacy of these biomarkers is limited, however, by the invasiveness of the associated procedures and limited physiological understanding of the GI system in health and functional disease.

Neural control of GI motility is primarily enacted by the enteric nervous system with additional input from the central nervous system via the vagus nerve.^{22,23} Extending from the brainstem to innervate various GI organs, the vagus nerve is a mixed sensory and cranial motor nerve that enables bi-directional transmission of afferent sensory information and efferent motor signals.²⁴ Vagal efferent fibers control innervated SMC via excitatory and

inhibitory transmission, which influence muscle tone and pacemaker activity in a spatially varying manner. For instance, vagal efferent pathways control gastric accommodation by modulating the tone of the fundus, as well as influencing gastric pacemaker activity, largely via ICC, affecting slow-wave amplitude but with minimal effects on frequency or antral tone.^{1,24} In pyloric musculature, dense vagal afferents are responsible for the transduction of localized mechanical signals (e.g., strain).²⁵ Additionally, vagal efferents in pyloric musculature suggest complex feedback mechanisms where the surrounding muscular wall acts as both a sensor and an effector.²⁶ These vagal efferent fibers are denser in the pylorus than the adjacent antrum, implying that the pyloric architecture has the potential for greater sensitivity. Compared to the stomach and pyloric sphincter, motility in the small intestine is primarily coordinated by the enteric nervous system with less influence from the central nervous system, though central activity may still modulate intestinal motility in response to physiological conditions.²⁷ Efferent fibers innervating the pylorus also maintain basal contractions via intrinsic myoelectrical tone, and relaxation is triggered by inhibitory vagal stimuli. Disruptions in vagal activity across the GDJ impair gastroduodenal coordination and delay gastric emptying^{28,29} and have been observed in cases where the vagus nerve is cut, either intentionally or not.^{30–32}

Erythromycin is a macrolide antibiotic with prokinetic effects due to its action as a motilin receptor agonist^{33,34} and influence on high-sensitivity neural receptors and low-sensitivity muscular receptors, including ICC.^{28,35,36} Indeed, work by Parkman et al. has highlighted that erythromycin's effect on gastric emptying rate is dose-dependent, with lower doses preferentially stimulating neural pathways and higher doses act directly on SMC.^{37,38} The prokinetic properties of erythromycin were discovered in the 1980s, which led to the development of non-antibiotic derivatives known as motilides.³⁹ Despite promising pre-clinical results, motilides were largely abandoned due to therapeutic inconsistency and their long QT effect. Motilides, however, are still of interest in research where they are readily available, cost-effective, and have known safety profiles. Additionally, erythromycin has demonstrated therapeutic value for patients with diabetic⁴⁰ and post-surgical (vagal damage) gastroparesis.³¹ Prior work by Sun et al.⁴¹ has provided insights into erythromycin's effect on body surface electrophysiological measurements; however, the *in vivo* porcine model presents an opportunity for a more direct and comprehensive understanding of this pharmaceutical agent on the gut. In the future, these agents may be utilized as supplemental diagnostic tools alongside validated tests, such as scintigraphy or body surface gastric mapping, to provide greater physiological insights.

In this study, we aimed to define the electromechanical effects of prokinetics and truncal vagotomy on the pylorus region by simultaneously measuring bioelectrical and mechanical activity from the GDJ in an in vivo anesthetized large animal model. We hypothesized that prokinetics would increase contractile frequency and strength, especially in the distal antrum, and that this would be associated with measurable bioelectrical changes. Additionally, we expected to see a reduced propensity for contraction across the stomach, pylorus, and duodenum following surgical vagotomy. We hypothesized that this response was also mediated via changes in bioelectrical patterns.¹⁷ The aims of this study were therefore twofold: firstly, to identify novel bioelectrical features of the gastroduodenal junction following macrolide prokinetic infusion and surgical vagotomy, which may inform clinical diagnostic tests, and secondly, to highlight potential therapeutic avenues for disorders of gut–brain interaction by identifying the relative roles of neural and hormonal activities on gastroduodenal electromechanical coupling.^{8,21}

2 | RESULTS

2.1 | Real-time observations

Electrophysiological mapping successfully captured slow waves and spikes in all animals over a period of (140 ± 22) min per pig that underwent a vagotomy and (67 ± 15) min per pig that did not. Positioning of the

EndoFLIP across the GDJ was performed successfully in all animals, and recordings were made from this region for (193 ± 60) min per pig that underwent prokinetic infusion but no vagotomy and (245 ± 23) min for each of the 5 pigs that underwent vagotomy. In each subject, the pylorus displayed the smallest luminal diameter at rest and during volatile contractions. Anecdotally, prokinetics promoted spiking and contraction of the terminal antrum and pyloric sphincter. These plainly visible contractions were synchronous with the conduction of antegrade gastric slow waves to the terminal antrum and with the audible gurgling of stomach contents. Prokinetics were associated with increased slow-wave propagation velocity and a reduction in pyloric quiescent zone width (Figures 1 and 2). Vagotomy was consistently associated with diminished slow-wave amplitude and velocity, decreased spike coverage, and low-amplitude contractions (Figure 2). Quantified values from control periods, prokinetic infusion, and post-vagotomy recordings are summarized in Table 1.

2.2 | Effect of prokinetics

During prokinetic infusion, changes in contractile signal amplitude were measured using high-resolution mapping and impedance planimetry in all pigs. Contractile signals expressed the greatest amplitude (58.7 ± 38.1) s after the beginning of the infusion and expressed significantly greater average amplitude than control recordings $([2.9 \pm 1.1]$ mm vs. $[2.2 \pm 0.9]$ mm; $p=0.002$). Amplitude increases in

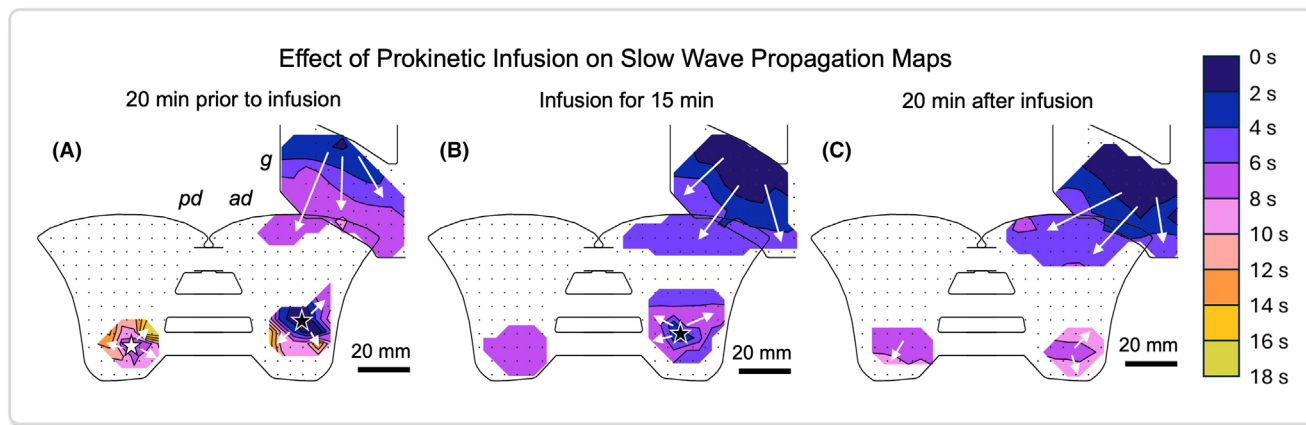


FIGURE 1 Effect of prokinetic infusion on slow-wave propagation profiles as measured from the same animal and period as Figures 3 and 4. In general, prokinetics increased gastric and duodenal slow-wave velocity without altering the propagation direction. (A) Propagation map for a typical slow wave 20 min prior to infusion with prokinetics. Arrows depict slow-wave depolarization direction. Black star; anterior proximal duodenal pacemaker region (i.e., where duodenal slow waves were first measured). White star; posterior proximal duodenal pacemaker acting independently and depolarizing a different region to the anterior proximal duodenal pacemaker. (B) Propagation map for a typical slow wave 15 min after the start of infusion. (C) Propagation map for a typical slow wave 20 min after the conclusion of the 60 min infusion. Each isochrone represents 2 s of propagation, as per the scale. Black dots represent electrode locations. *ad*, anterior duodenal electrode; *g*, gastric electrode; *pd*, proximal duodenal electrode.

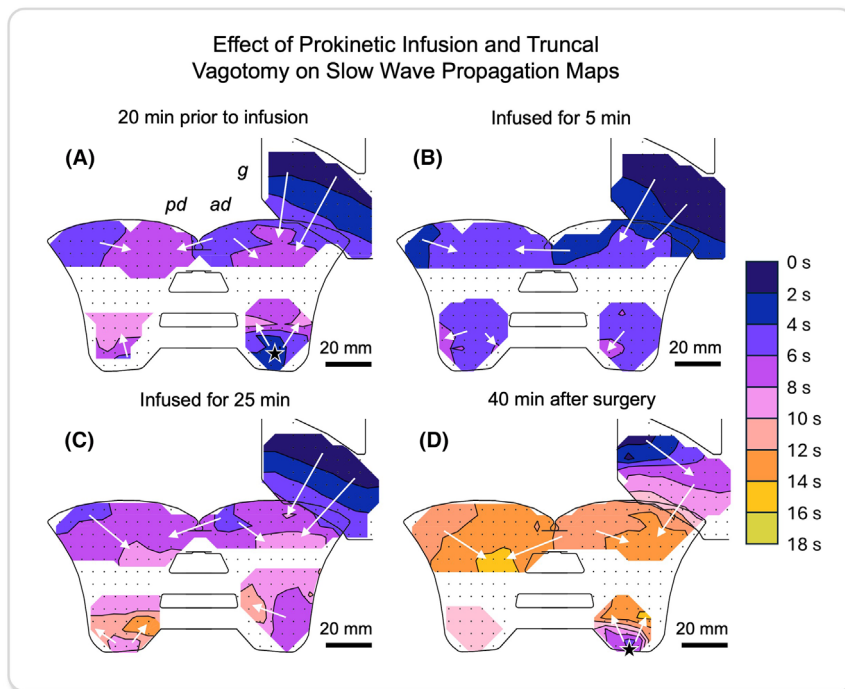


FIGURE 2 Effect of prokinetic infusion and truncal vagotomy on slow-wave propagation profiles as measured from the same animal and period as [Figures 5](#) and [6](#). In general, prokinetics increased gastric and duodenal slow-wave velocity without altering the propagation direction. Conversely, vagotomy decreased propagation velocity of both gastric and duodenal slow waves and displaced the gastric pacing region toward the greater curvature (outside of mapped area). (A) Propagation map for a typical slow wave 20 min prior to infusion with prokinetics. Arrows depict slow-wave depolarization direction. Black star; anterior proximal duodenal pacemaker region (i.e., where duodenal slow waves were first measured). (B) Propagation map for a typical slow wave 5 min after the start of infusion. (C) Propagation map for a typical slow wave 25 min after the start of infusion. (D) Propagation map for a typical slow wave 40 min after the conclusion of the 60 min infusion. Each isochrone represents 2 s of propagation, as per the scale. Black dots represent electrode locations. *ad*, anterior duodenal electrode; *g*, gastric electrode; *pd*, proximal duodenal electrode.

Parameter	Control (<i>N</i> = 10)	Prokinetics (<i>N</i> = 10)	Vagotomy (<i>N</i> = 5)
Slow-wave RMS amplitude (mV)	0.99 ± 0.31	1.21 ± 0.31	0.70 ± 0.14
Dominant gastric slow-wave frequency (cpm)	5.4 ± 3.7	5.0 ± 1.8	6.3 ± 1.6
Dominant duodenal slow-wave frequency (cpm)	16.9 ± 4.0	17.2 ± 4.8	18.7 ± 0.25
Spike RMS amplitude (mV)	0.24 ± 0.04	0.28 ± 0.05	0.24 ± 0.15
Spike coverage (%)	66.1 ± 16.2	66.1 ± 21.4	44.8 ± 25.0
Contraction RMS amplitude (mm)	2.2 ± 0.9	2.9 ± 1.1	1.2 ± 0.6
Distensibility index (mm ² mmHg ⁻¹)	2.4 ± 1.4	2.5 ± 1.4	5.1 ± 6.2

TABLE 1 Parameters quantified from electrophysiological and impedance planimetry recordings. All measures are means ± SD.

this manner were most pronounced in the distal antrum (30–60 mm proximal to the pyloric sphincter; [Figure 3A](#)). During prokinetic infusion, slow-wave signal amplitudes increased significantly compared to baseline ([1.21 ± 0.31] mV vs. [0.99 ± 0.31] mV; $p = 0.034$; [Figure 4](#)). Similarly,

spike signals contained significantly greater amplitude during this period ([0.28 ± 0.05] mV vs. [0.24 ± 0.04] mV; $p = 0.005$), although their spatial characteristics appeared unchanged—there were no changes in patch coverage across the high-resolution electrode arrays ([66.1 ± 16.2]

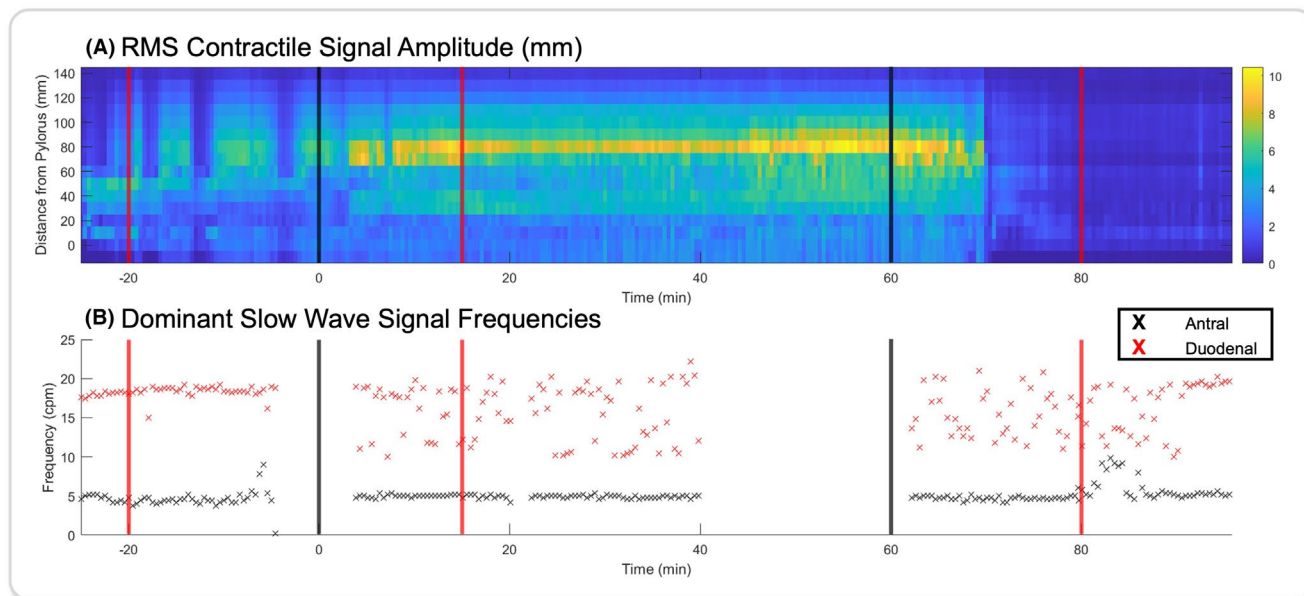


FIGURE 3 Typical electromechanical profile across the gastroduodenal junction following prokinetic infusion, exemplified in one pig. (A) During prokinetic infusion (0–60 min; black lines), contractile signal amplitude increased in the antrum (~80 mm proximal to the pylorus) for the duration of the infusion and 10 min following. (B) Over the same period, there were changes in the gastric and duodenal dominant frequencies associated with prokinetics—gastric signals had reduced variation, while intestinal signals had greater variation. Absence of data indicates a period where no recordings were taken. Red lines indicate time points sampled for [Figures 1](#) and [4](#).

% vs. $[66.1 \pm 21.4]$ %; $p=0.796$). In 8/10 pigs, there was a “pause” in contractile activity during the prokinetic infusion, during which there was a sudden and significant reduction in amplitude ($[0.8 \pm 0.2]$ mm vs. $[2.9 \pm 1.1]$ mm; $p < 0.001$). These periods, herein termed “contractile quiescence,” lasted (17.2 ± 9.4) min before the GDJ returned to a pattern of functional contractions. [Figure 3](#) demonstrates a typical electromechanical profile before, during, and after prokinetic infusion in a pig that did not express contractile quiescence, whereas [Figure 5](#) demonstrates a typical electromechanical profile in which a period of contractile quiescence occurred between ~10 and 40 s.

During control recordings, gastric slow waves were measured with a dominant frequency of (5.4 ± 3.7) cpm, which was significantly different from those observed in duodenal slow waves ($[16.9 \pm 4.0]$ cpm; $p < 0.001$) ([Figure 3B](#)). During prokinetic infusion, gastric signals demonstrated an insignificant change in mean dominant frequency but reduced variation ($[5.0 \pm 1.8]$ cpm). Similarly, dominant duodenal slow-wave frequencies measured during prokinetic infusion had slightly elevated variation compared to control recordings, but there was no change in mean ($[17.2 \pm 4.8]$ cpm) ([Figure 3B](#)).

significantly from (2.9 ± 1.1) mm to (1.2 ± 0.6) mm ($p=0.049$). In 3/5 pigs, contractile amplitude was lowest at the pylorus (exemplified in [Figure 5A](#)), and in 2/5 pigs, contractile activity was lowest in the adjacent antrum and duodenum. Contractile changes were associated in these subjects with a decrease in average slow-wave signal amplitude from (0.88 ± 0.21) mV to (0.70 ± 0.14) mV ($p=0.039$; [Figure 6A–D](#)). Vagotomy was associated with a significant increase in dominant duodenal slow-wave frequencies, ($[18.7 \pm 0.25]$ cpm vs. $[17.2 \pm 1.9]$ cpm; $p < 0.001$). Over this period, dominant gastric slow-wave frequencies increased, although this change was not statistically significant ($[6.3 \pm 1.6]$ cpm vs. $[5.4 \pm 3.7]$ cpm; $p=0.373$). Additionally, there was a significant decrease in spike coverage ($[65.4 \pm 21.5]$ % vs. $[44.8 \pm 25.0]$ %; $p < 0.001$; [Figure 6E–H](#)) across the high-resolution electrical arrays, and the spikes that were measured displayed only an insignificant increase in amplitude from (0.21 ± 0.03) mV to (0.24 ± 0.15) mV ($p=0.643$). Mean pyloric distensibility index was not significantly different after prokinetic infusion or surgical vagotomy and was measured with high variance throughout recordings ([Table 1](#)).

2.3 | Effect of truncal vagotomy

Following completion of the truncal vagotomy in 5 pigs, the subjects’ average contractile amplitude diminished

3 | DISCUSSION

The present study documents the effect of prokinetic infusion and surgical vagotomy on the electromechanical

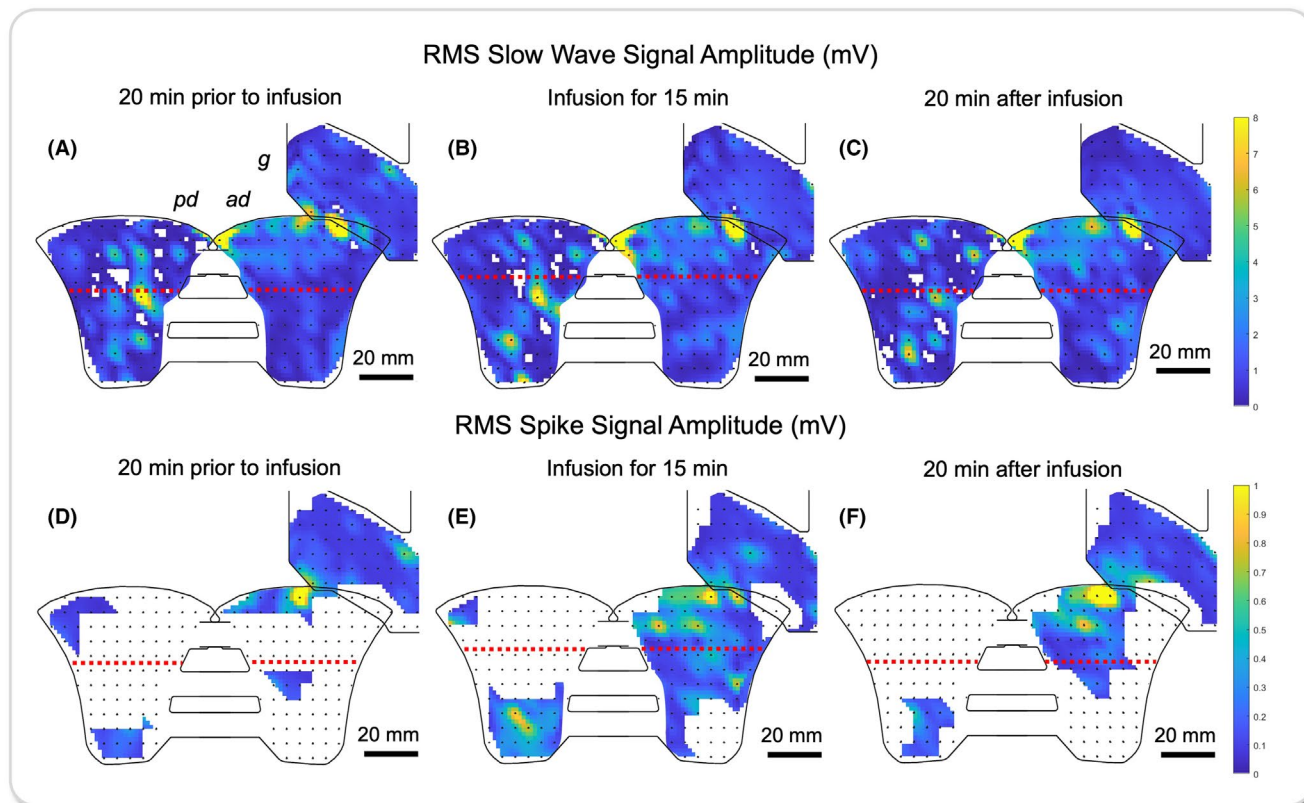


FIGURE 4 Slow-wave and spike signal amplitude as measured from the same animal and period as Figures 1 and 3. (A–C) Slow-wave signals from the anterior (*ad*) and posterior (*pd*) duodenum increase in amplitude during prokinetic infusion. (D–F) In this pig, spike patches were more widespread during prokinetic infusion, compared to before and after the intervention, although this behavior was not common to all subjects. There were less remarkable changes in slow-wave and spike signals in the gastric antrum (*g*) than the duodenum. Black dots represent electrode locations and red lines denote the middle of the pylorus during this recording.

activity of the porcine GDJ. Simultaneous high-resolution electrical mapping and impedance planimetry techniques successfully measured bioelectrical and contractile patterns across the GDJ in 10 pigs. In all pigs, the pylorus demarcated the antrum and duodenum mechanically (via minimal lumen diameter) and electrically (by insulating gastric and intestinal slow waves). There were notable differences in electromechanical activity from recordings in control periods, during prokinetic infusion, and following truncal vagotomy, thereby demonstrating the mechanistic influence of prokinetics and vagal innervation in this GDJ region. In general, prokinetics served to promote terminal antral contractions, mediated through significant increases in slow-wave and spike amplitudes and by reduced variability of dominant gastric slow-wave signals. This supports an initial hypothesis—that erythromycin alters GDJ motility via changes in electrophysiological behavior. Together, these features characterize a high-amplitude, highly coordinated bioelectrical stimulus, which has been shown to increase motility in the intact GI system.^{17,41,42} Contrasting the effects of prokinetics, truncal

vagotomies were associated with diminished contractile signal amplitude, resulting from a reduction in slow-wave signal amplitude and reduced coverage of spiking across the electrode arrays. Interestingly, vagotomies were associated with increased dominant slow-wave frequencies in both the antrum and duodenum, as well as a reduction in variability of these frequencies—indicating more frequent and coordinated slow-wave behavior across the junction.

The documented modulation of slow-wave frequency following prokinetic and vagotomy interventions is likely a result of the underlying biophysical nature of slow waves.⁴³ During prokinetic infusion, gastric slow-wave amplitude increased, concomitantly increasing velocity and period (Table 1 and Figure 4), as was previously observed by Sun et al.⁴¹ The converse is true for post-vagotomy data—a decrease in slow-wave amplitude resulted in decreased velocity and period, as has been noted by others²⁸ (Table 1 and Figure 2). However, Mathis and Malbert reported a contrasting result when using erythromycin and vagal cooling in anesthetized pigs, where vagal cooling led to reduced

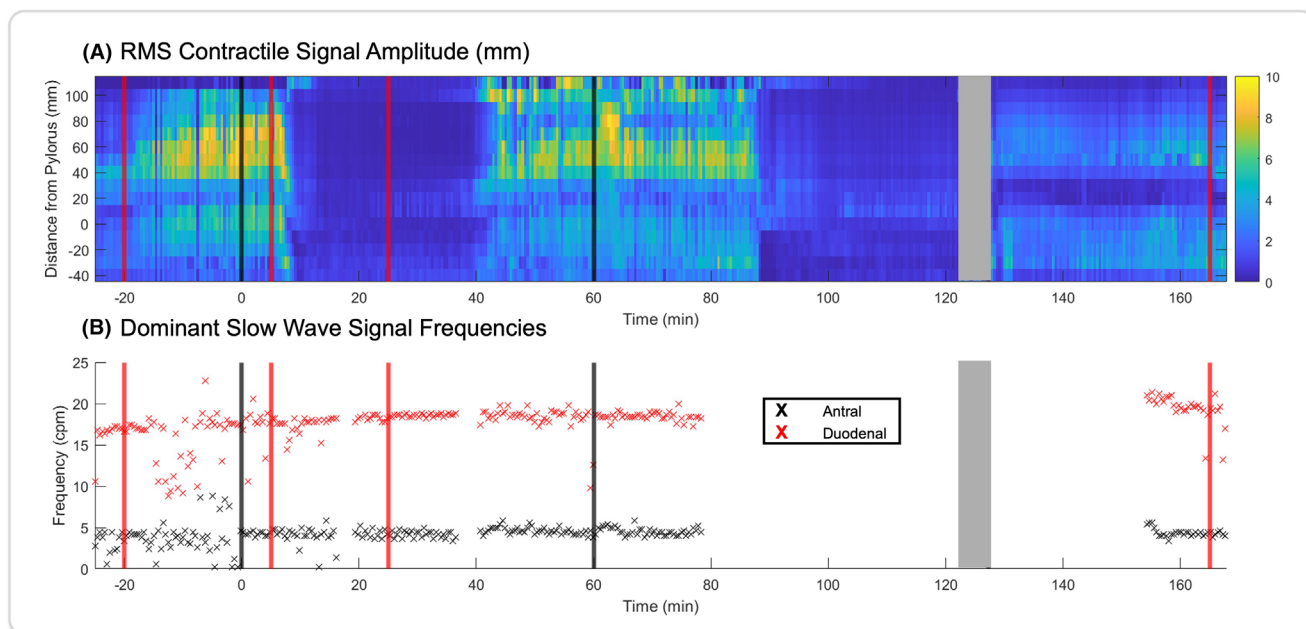


FIGURE 5 Electromechanical profile across the gastroduodenal junction following prokinetic infusion and surgical vagotomy, exemplified in one pig. (A) During prokinetic infusion (0–60 min; black lines) contractile signal amplitude increased in the antrum (~80 mm proximal to the pylorus) for the duration of the infusion and 15 min following. Contractile quiescence was observed from 10 to 40 min across the entirety of the junction. Following vagotomy (gray period), contractile activity in the stomach and duodenum slightly increased, while motion of the pylorus was diminished. (B) Simultaneous with (A), prokinetics were associated with decreased variability in dominant slow-wave frequencies in the antrum and duodenum. Red lines indicate time points sampled for [Figures 2](#) and [6](#).

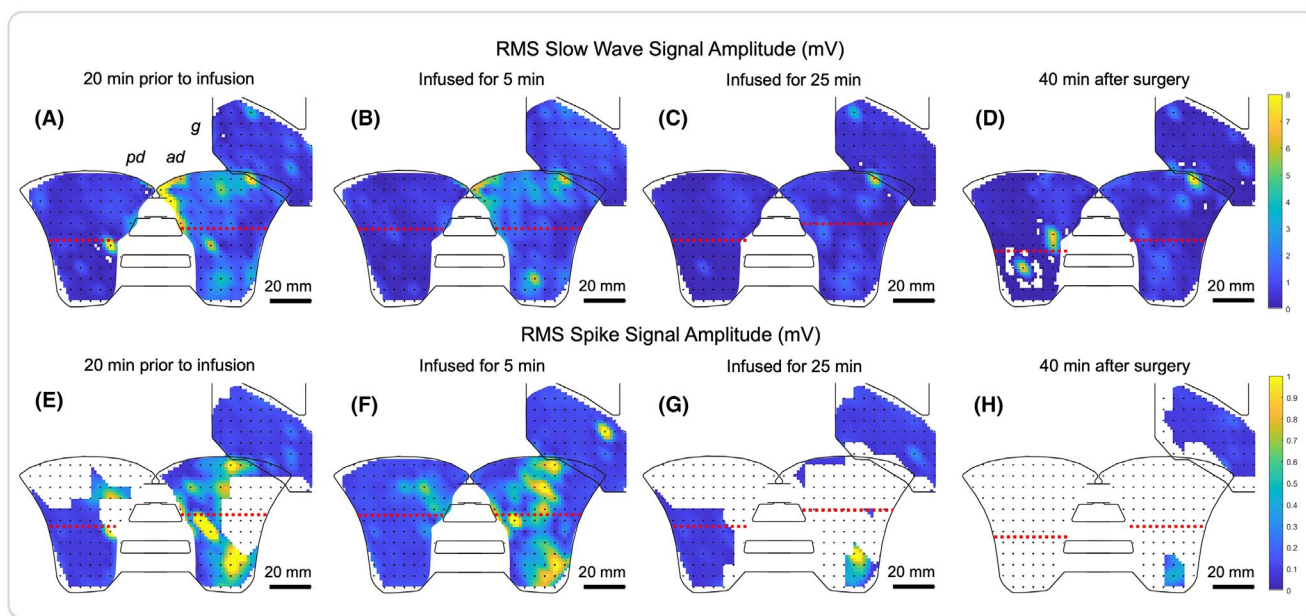


FIGURE 6 Slow-wave and spike signal amplitude as measured from the same animal and period as [Figures 2](#) and [5](#). (A, B) Slow-wave signal amplitude increased during prokinetic infusion, mirroring contractile signal amplitude ([Figure 1](#)). (C, D) During contractile quiescence and following surgical vagotomy, slow-wave signal amplitude decreased significantly. (E, F) Prokinetics increased spike patch coverage compared to control. (G, H) Spike patches were less prevalent during contractile quiescence and after surgical vagotomy. Black dots represent electrode locations and red lines denote the middle of the pylorus during this recording.

gastric emptying—not through a decrease in contractile amplitude, as observed in the present study, but via an increase in pyloric tone.³⁶ While these physiological responses result in the same functional outcome—delayed gastric emptying—they differ mechanistically, likely driven by disparities in experimental design, such as the reduced erythromycin dosage and lack of a prokinetic washout period prior to vagal interventions by Mathis and Malbert. An earlier study by these authors, which utilized anesthetized pigs but not erythromycin, suggests that the washout period was particularly influential, as surgical vagotomy reduced antral contractile amplitude.²⁸ These observations indicate that the mechanical effects of both interventions are caused by modulation of either slow-wave amplitude or frequency, both of which are regulated, in part, by the underlying ICC–MP network.

Studies of electromechanical coupling in humans,^{4,44} pigs,^{17,45} and other animal models^{42,46,47} have observed a functional relationship between slow waves and contractions, and the present data provide further support for these observations. The documented results suggest that slow-wave amplitude works in tandem with slow-wave variability to define the contractile state of the GDJ via modulation of spikes, contractions, and ultimately, gastric emptying. The dosage of erythromycin in this study ($1 \text{ mg} \cdot \text{kg}^{-1}$) suggests that these effects result from stimulation of both neurogenic and myogenic pathways.^{37,38} In theory, stronger, more consistent slow waves promote the generation of spike patches with greater amplitude and coverage to promote contractions during prokinetic administration. Indeed, this theory is consistent with magnetogastrography⁴⁸ and electrogastrography⁴⁹ measurements in humans, suggesting that the mechanical effects of this prokinetic are functionally mediated via electromechanical coupling. Notably, Chen et al. found that erythromycin increased the variability of gastric slow-wave frequency in humans, which contrasts with the present results.⁴⁹ These conflicting observations could result from differences in measurement technique (mapping from the serosal surface vs. abdominal surface) or dosage (1 vs. $6 \text{ mg} \cdot \text{kg}^{-1}$). We did observe an increase in small intestinal slow-wave variability in some subjects during prokinetic administration (i.e., Figure 3), which may explain the conflicting evidence—cutaneous recordings capture information from a large area which inevitably includes information from the small intestine. The spatial resolution of direct serosal measurements highlights an advantage of region-specific high-resolution electrical mapping over other non-invasive measurement techniques, particularly in a research environment.

Contractile quiescence following prokinetic infusion was an unexpected result that does not appear in other studies that have used erythromycin to study the GDJ.⁴¹

It is hypothesized that contractile quiescence results from innate physiological feedback mechanisms, such as motilin receptor desensitization⁵⁰ or enteric nervous system feedback.²² The unpredictability of this behavior, particularly regarding the inter-individual variability, may limit the diagnostic and therapeutic utility of erythromycin clinically if contractile quiescence manifests similarly in humans. Ultimately, these speculative underlying relationships require additional studies into the mechanisms and potential physiological impact of the observed contractile quiescence, which can now be designed using these present techniques and results as a foundation. In particular, *in vitro* studies will provide a perspective independent of external influence, such as central nervous stimuli.

The vagus nerve serves to facilitate communication between the central nervous system and the GI system, where parasympathetic inhibitory signals—in tandem with hormones and the enteric nervous system—induce pyloric relaxation and promote gastric emptying.²⁸ Surgical vagotomy removes this stimulus from the gastroduodenal region and is associated with poor gastric emptying, abdominal symptoms, and inhibited GDJ motility, as has been observed in procedures such as esophagectomy^{32,51} and is confirmed by the current results. The observed decrease in motor activity across the GDJ is likely the result of several physiological changes, including (i) decreased sensory feedback from pyloric afferents,²⁵ (ii) decreased parasympathetic stimuli and SMC tone,²⁶ and (iii) changes in Ca^{2+} sensitivity, via altered neural input to the functional myoelectrical unit.²⁴ Here, it is shown that truncal vagotomy alters the underlying electrophysiological behavior of the GDJ, highlighting the role of the vagus in regulating bioelectrical activity of the GDJ and a potential pathophysiological mechanism for patients with post-surgical gastroparesis.

The present data show that the vagus nerve controls motility through modulation of bioelectrical activity, and that surgical vagotomies may alter gastroduodenal motility within minutes, suggesting that these changes are independent of underlying structural or anatomical changes (e.g., diabetic ICC depletion⁴) which would take greater time to manifest. These observations support prior findings that vagotomy-induced gastroduodenal dysfunction is mediated through electrophysiological mechanisms rather than via changes in calcium sensitivity or SMC contractility alone. While this concept has been widely suggested by the literature to date,^{28,29} the present study provides a new level of technical and spatial detail, confirming these effects in greater spatiotemporal resolution and highlighting how vagotomy can rapidly alter motility of the GDJ within minutes.^{28,29} Additionally, it seems that the vagus nerve may alter, via modulation of

intrinsic slow-wave frequencies, entrainment of the stomach by the dominant gastric pacemaker region (Figure 6); thus, changes in neurological stimuli may result in dysrhythmic or retrograde slow-wave behavior, often associated with nausea and vomiting.^{52,53}

Clinical use of the EndoFLIP in the pylorus is typically limited to a few minutes and primarily assesses the distensibility index.³ Anecdotally, accurate assessment of the pylorus in this manner would require several minutes of recording—to ensure that all motor patterns (i.e., terminal antral contractions) are captured¹⁷—though this time would theoretically be shorter during prokinetic infusion due to greater contractile consistency and strength (Figure 3A) and longer for those with vagal disruptions for similar reasons (Figure 5A).

Actionable biomarkers are considered an important milestone for the development of accurate clinical diagnostic and treatment protocols, especially for disorders of gut–brain interaction, which are currently categorized by symptomatic score rather than by organic cause.^{8,9} Ultimately, the translation of these techniques from animal studies to humans is required to determine their suitability in a clinical environment and should be the focus of future efforts. There are, however, limitations in the present study that make this translation challenging. Firstly, the development of minimally invasive electromechanical measurement tools should be prioritized—prokinetic therapy could be considered in combination with minimally invasive impedance planimetry (e.g., EndoFLIP),¹⁹ electrogastrography (e.g., body surface gastric mapping),⁵⁴ or endoscopic electrical mapping¹² to expand clinical diagnostic capabilities and further our understanding of the GDJ in health and disease. The addition of simultaneous heart rate variability measurement would enable the calculation of sympathetic and parasympathetic activity, providing another pathological perspective and bolstering the pool of possible diagnostic tools for GI clinicians.⁵⁵ Under these conditions, observations could capture possible changes in bioelectrical slow-wave rhythmicity or contractile profile in response to prokinetic administration. It is plausible that, given a substantial cohort, subcategories of these patients could be identified from these measurable markers, and several phenotypes may start to present themselves. For example, for patients with ICC degeneration and loss of network structure (as is common in aging⁵⁶ and gastroparetic patients^{4,53,57}), prokinetics may not induce significant changes in slow-wave amplitude and rhythmicity. In comparison, a significant electrophysiological response to prokinetics may suggest that a patient's symptoms are related to hormonal, neural, or muscular pathologies that impede electromechanical transduction and Ca^{2+} sensitivity. Indeed, another prokinetic agent, cisapride, has been documented to promote proximal gastric motility and improve

gastric emptying rate in patients with progressive systemic sclerosis, but not in patients with insulin-dependent diabetes mellitus, irrespective of the fact that both pathologies are associated with poor gastric emptying.⁵⁸ The second limitation of the present study is evident here—the electromechanical effects of other common prokinetic agents, such as cisapride, metoclopramide, or domperidone, should also be investigated, as these may prove to be more clinically suitable than erythromycin (which is accompanied with the risk of antibiotic resistance). Finally, the mixed-protocol nature of this study may influence the present results (i.e., each pig that underwent a vagotomy had previously been dosed with intravenous erythromycin), although this seems unlikely given that the measurable electromechanical effects of erythromycin dissipated prior to the commencement of surgical vagotomy and the long duration of post-vagotomy recordings. In the future, the development of minimally invasive measurement tools will enable the translation of these techniques to humans, where phenotypic profiles of different disorders of gut–brain interaction may be elucidated.

4 | MATERIALS AND METHODS

4.1 | Animal preparation

Following ethical approval from the University of Auckland Animal Ethics Committee (AEC25159), in vivo experiments were performed on fasted female crossbreed weaner pigs ($N=10$; 42.8 ± 4.1 kg; mean \pm SD). Female pigs were used because they require less manipulation to perform intra-operative electrophysiological measurements, and there are fewer surgical risks involved. Baseline physiological characteristics of this cohort have been published previously.¹⁷ In short, anesthesia was induced with zolazepam and tiletamine (0.1 mL kg^{-1} , Zoletil, Virbac, NZ) and maintained with propofol (Diprivan 2%, $0.2\text{--}0.4 \text{ mg kg}^{-1} \text{ min}^{-1}$; AstraZeneca, UK).⁵⁹ Monitoring of vital signs confirmed that they were maintained within normal physiological ranges. A midline laparotomy exposed the gastroduodenal serosa. All pigs underwent simultaneous electrical and impedance planimetry measurements before being euthanized via a bolus injection of sodium pentobarbital while still under anesthesia.

4.2 | High-resolution electrical mapping

High-resolution electrical mapping followed techniques previously described.^{14,17} Briefly, flexible anatomically specific electrode cradles housing custom flexible printed electrode arrays (256 electrodes, 5 mm interelectrode spacing) were

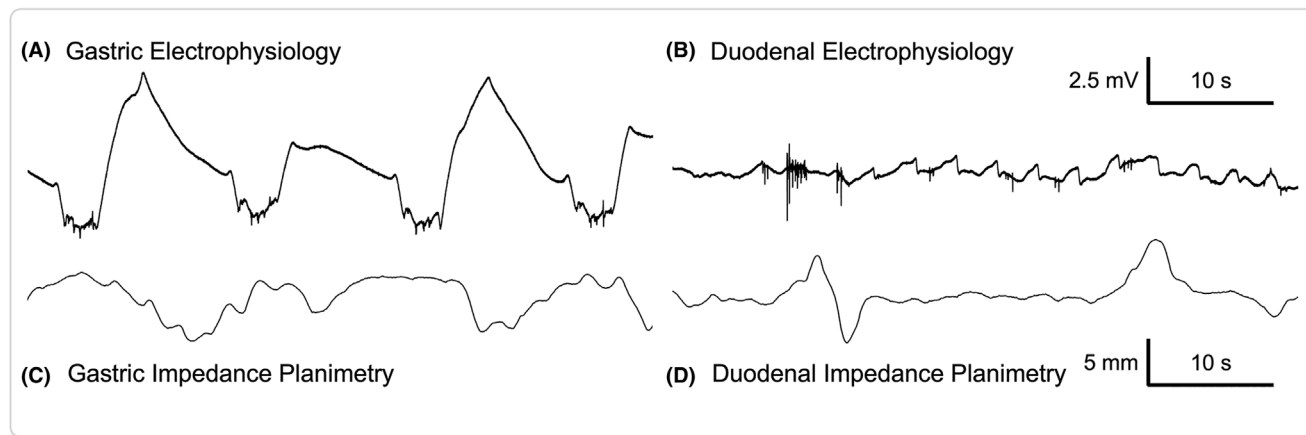


FIGURE 7 Simultaneous electrical and impedance planimetry recordings across the gastroduodenal junction. (A, B) Electrophysiological signals from the gastric antrum and proximal duodenum. (C, D) Impedance planimetry signals from the gastric antrum and proximal duodenum.

positioned on the gastroduodenal serosa. These electrode arrays were connected to an electrophysiological mapping system (ActiveTwo, BioSemi, The Netherlands) and were recorded at 512 Hz. Electrical signals from the GDJ were visualized and exported for future analysis (Figure 7A,B).

4.3 | Impedance planimetry

To record luminal contour, an EndoFLIP impedance planimetry catheter (EF-322N, Medtronic, USA) was orally inserted into the stomach and passed into the duodenum, where it was positioned across the pylorus. In eight animals, the catheter tip was clamped to the small intestine, ~5 cm distal to the measurement site, to prevent migration during inflation. Catheter inflation volumes of 40 mL and 50 mL were informed by previous investigations⁶⁰ and prior experience, and optimal contours were confirmed using a baseline distensibility test. Following inflation, EndoFLIP positioning across the pylorus was confirmed via manual compression and observation of the typical hourglass contour.¹⁷ Luminal diameter was estimated at 16 points along the balloon length from a series of electrodes (16 × 1, 10 mm apart) with a sampling frequency of 10 Hz. Data were continually recorded throughout the duration of the study and transferred to a hard drive for later visualization and analysis (Figure 7C,D). Distensibility indices for control, prokinetic, and vagotomy recordings were calculated for comparison.

4.4 | Prokinetic infusion

Following control recording periods, each pig was intravenously infused with Erythromycin (Erythromycin

lactobionate, lot #25277TB22, Amdipharm, UK). In 9 of 10 pigs, a dose of 1 mg kg⁻¹ was mixed with 40 mL of saline and infused at a rate of 0.667 mL min⁻¹. In one pig, a greater dose (2 mg kg⁻¹) was used with the intent of investigating any dose-dependent effects, although this protocol was not repeated due to an elevation in heart rate. Dosages were informed by prior studies.^{34,61}

4.5 | Truncal vagotomy

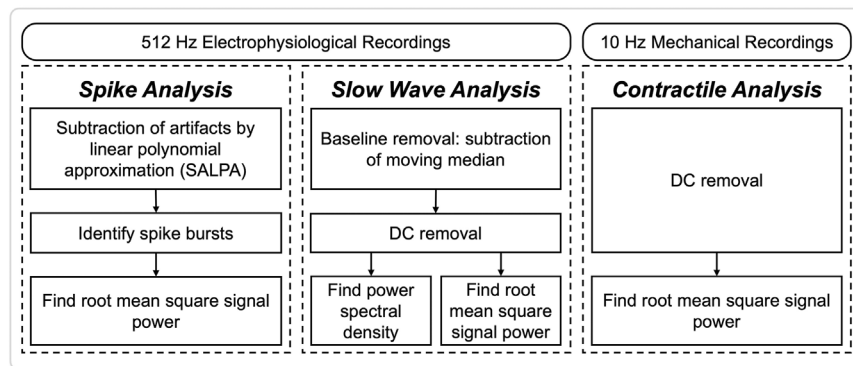
To ascertain the extent of vagal input to the gastroduodenal electromechanical coupling, 5 pigs underwent a truncal vagotomy (55.7 ± 12.9 min) following the conclusion of their prokinetic infusion. The use of prokinetics to stimulate gastrointestinal motility was expected to exemplify the effects of surgical vagotomy more clearly. To perform this procedure, the lower esophagus was exposed through an incision at the gastroesophageal junction, and the anterior and posterior vagal trunks were identified and transected with sharp dissection. The stomach was replaced, and the electrophysiological and impedance planimetry systems were corrected for displacement.

Electrophysiological signal measurements were not continuous during the prokinetic infusion period, and following the surgical vagotomy, due to data storage limitations.

4.6 | Analysis pipeline

Electrical signals containing slow waves and spikes were consistently measured from the gastroduodenal serosa in all pigs. Slow waves and spikes had unique morphology, as previously described,^{14,17} and were thus analyzed independently. Electrophysiological signals were prepared for

FIGURE 8 Analysis pipeline flowchart. Left: Electrophysiological signals, sampled at 512 Hz, were analyzed for both slow-wave and spike content. Right: Mechanical signals recorded using impedance planimetry at 10 Hz.



slow-wave quantification by removing baseline drift and DC components and were prepared for spike quantification using a Subtraction of Artifacts by Linear Polynomial Approximation (SALPA) filter (Figure 8). Impedance planimetry signals, captured from the EndoFLIP, were prepared for quantification by removing the DC component. Signals were prepared in this manner to minimize noise and optimize signal quality by tailoring filters to specific events.

Once prepared, electrical and mechanical signals were analyzed in the time domain; signal amplitude was quantified by computing the root mean square (RMS) of each sample set (80s each) (Figure 8). Electrophysiological signals were also transformed into the frequency domain and expressed in terms of their power spectral density to identify frequency characteristics of gastric and intestinal slow-wave signals. Spikes were analyzed in the time domain only, as the frequency characteristics of SALPA-filtered signals do not vary with changes in spike intensity. Frequency bins of maximum power density in the power spectrum of antral and duodenal slow-wave signals were calculated for comparison to mechanical signal amplitude. Electrophysiological signals from time points of interest (e.g., before, during, and after prokinetic infusion) were sampled from each animal for further high-resolution analysis. Optimally filtered slow-wave data were visualized as isochrone plots using a validated, automated algorithm in GEMS, as has been previously described,^{17,62} to enable qualitative assessment of slow-wave patterns.

4.7 | Statistics

All quantitative comparisons were characterized using Student's *t*-test, except for spike coverage calculations, which instead used the Wilcoxon signed-rank test due to limited sample sizes. A significance threshold of $p < 0.05$ was used for interpretation of all results. Quantified values are presented as mean \pm standard deviation (SD).

5 | CONCLUSIONS

This study presents a novel perspective on the GDJ in response to erythromycin (prokinetic) infusion and truncal vagotomy. Compared to control recordings, erythromycin infusion increased the amplitude of slow waves, spikes, and contractions across the entire junction, and more consistent gastric slow-wave rhythms were measured. In contrast, surgical vagotomy immediately decreased contractile patterns and reduced bio-electrical activity. Prokinetic therapy may be combined with minimally invasive measurements, such as the EndoFLIP, to further identify clinical biomarkers of GDJ health and disease.

AUTHOR CONTRIBUTIONS

Sam Simmonds: Conceptualization; writing – original draft; methodology; visualization; writing – review and editing. **Tim H.-H. Wang:** Methodology; writing – review and editing. **Ashton Matthee:** Writing – review and editing; methodology. **Jarrah M. Dowrick:** Methodology; writing – review and editing. **Andrew J. Taberner:** Writing – review and editing. **Peng Du:** Writing – review and editing; conceptualization. **Timothy R. Angeli-Gordon:** Conceptualization; funding acquisition; methodology; writing – review and editing.

ACKNOWLEDGMENTS

We thank Ms. Linley Nisbet for her expert assistance with the in vivo studies and Dr. Sachira Kuruppu for his assistance with the spike analysis algorithm. Funding for this project was received from a Marsden Fund and a Rutherford Discovery Fellowship from the Royal Society Te Apārangi. Open access publishing facilitated by The University of Auckland, as part of the Wiley - The University of Auckland agreement via the Council of Australian University Librarians.

CONFLICT OF INTEREST STATEMENT

All authors have no conflicts of interest to declare.

DATA AVAILABILITY STATEMENT

The data that support the findings of this study are available from the corresponding author upon reasonable request.

ORCID

Sam Simmonds  <https://orcid.org/0000-0003-0095-7235>

Tim H.-H. Wang  <https://orcid.org/0000-0001-6200-2384>

Ashton Matthee  <https://orcid.org/0000-0002-5277-6965>

Jarrah M. Dowrick  <https://orcid.org/0000-0002-6674-6548>

Timothy R. Angeli-Gordon  <https://orcid.org/0000-0003-1610-3787>

REFERENCES

- Goyal RK, Guo Y, Mashimo H. Advances in the physiology of gastric emptying. *Neurogastroenterol Motil.* 2019;31:e13546.
- Kelly KA. Gastric emptying of liquids and solids: roles of proximal and distal stomach. *Am J Phys.* 1980;239:71-76.
- Soliman H, Gourcerol G. Targeting the pylorus in gastroparesis: from physiology to endoscopic pyloromyotomy. *Neurogastroenterol Motil.* 2023;35:e14529.
- O'Grady G, Angeli TR, Du P, et al. Abnormal initiation and conduction of slow-wave activity in gastroparesis, defined by high-resolution electrical mapping. *Gastroenterology.* 2012;143:589-593.
- Ukleja A. Dumping syndrome: pathophysiology and treatment. *Nutr Clin Pract.* 2005;20:517-525.
- Talley NJ, Locke GR, Lahr BD, et al. Functional dyspepsia, delayed gastric emptying, and impaired quality of life. *Gut.* 2006;55(7):933-939.
- Broeders BW, Carbone F, Balsiger LM, et al. Review article: functional dyspepsia—a gastric disorder, a duodenal disorder or a combination of both? *Aliment Pharmacol Ther.* 2023;6:1-10.
- Camilleri M, Chedid V. Actionable biomarkers: the key to resolving disorders of gastrointestinal function. *Gut.* 2020;69:1730-1737.
- Dowrick JM, Roy NC, Bayer S, et al. Unsupervised machine learning highlights the challenges of subtyping disorders of gut-brain interaction. *Neurogastroenterol Motil.* 2024;36:e14898.
- Huizinga JD, Lammers WJEP. Gut peristalsis is governed by a multitude of cooperating mechanisms. *Am J Physiol Gastrointest Liver Physiol.* 2009;296:1-8.
- O'Grady G, Angeli TR, Paskaranandavadivel N, et al. Methods for high-resolution electrical mapping in the gastrointestinal tract. *IEEE Rev Biomed Eng.* 2018;12:287-302.
- Tremain P, Chan CH, Rowbotham D, et al. Endoscopic mapping of bioelectric slow waves in the gastric antrum. *Device.* 2024;2:100292.
- Parsons SP, Huizinga JD. Phase waves and trigger waves: emergent properties of oscillating and excitable networks in the gut. *J Physiol.* 2018;596:4819-4829.
- Simmonds S, Cheng LK, Ruha WW, Taberner AJ, Du P, Angeli-Gordon TR. Measurement and analysis of in vivo gastroduodenal slow wave patterns using anatomically-specific cradles and electrodes. *IEEE Trans Biomed Eng.* 2023;71:1287-1297.
- Lin Q, Qin M, Zhao SG, et al. The roles of PDGFR α signaling in the postnatal development and functional maintenance of the SMC-ICC-PDGFR α cell (SIP) syncytium in the colon. *Neurogastroenterol Motil.* 2019;31:1-12.
- Lammers WJEP. Propagation of individual spikes as 'patches' of activation in isolated feline duodenum. *Am J Physiol Gastrointest Liver Physiol.* 2000;278:G297-G307.
- Simmonds S, Matthee A, Dowrick JM, Taberner AJ, Du P, Angeli-Gordon TR. Electromechanical coupling and anatomy of the in-vivo gastroduodenal junction. *Am J Physiol Gastrointest Liver Physiol.* 2024;327:G93-G104.
- Lammers WJEP, Slack JR. Of slow waves and spike patches. *News Physiol Sci.* 2001;16:138-144.
- Malik Z, Sankineni A, Parkman HP. Assessing pyloric sphincter pathophysiology using EndoFLIP in patients with gastroparesis. *Neurogastroenterol Motil.* 2015;27:524-531.
- Janssen P, Leuven KU, Harris MS, Masaoka T, Farré R. The relation between symptom improvement and gastric emptying in the treatment of diabetic and idiopathic gastroparesis. *Am J Gastroenterol.* 2013;108:1382-1391.
- Camilleri M. Relationship of motor mechanisms to gastroparesis symptoms: toward individualized treatment. *Am J Physiol Gastrointest Liver Physiol.* 2021;320:G558-G563.
- Furness JB. The enteric nervous system and neurogastroenterology. *Nat Rev Gastroenterol Hepatol.* 2012;9:286-294.
- Sharkey KA, Mawe GM. The enteric nervous system. *Physiol Rev.* 2023;103:1487-1564.
- Chang HY, Mashimo H, Goyal RK. Musings on the wanderer: what's new in our understanding of vago-vagal reflex? IV. Current concepts of vagal efferent projections to the gut. *Am J Physiol Gastrointest Liver Physiol.* 2003;284:G357-G366.
- Kraichely RE, Farrugia G. Mechanosensitive ion channels in interstitial cells of Cajal and smooth muscle of the gastrointestinal tract. *Neurogastroenterol Motil.* 2007;19:245-252.
- Powley TL, Hudson CN, JL MA, et al. Organization of vagal afferents in pylorus: mechanoreceptors arrayed for high sensitivity and fine spatial resolution? *Auton Neurosci.* 2014;2:36-48.
- Browning KN, Travagli RA. Central nervous system control of gastrointestinal motility and secretion and modulation of gastrointestinal functions. *Compr Physiol.* 2014;4:1339-1368.
- Malbert CH, Mathis C, Laplace JP. Vagal control of pyloric resistance. *Am J Physiol Gastrointest Liver Physiol.* 1995;269:G558-G569.
- Hall KE, El-Sharkawy TY, Diamant NE. Vagal control of canine postprandial upper gastrointestinal motility. *Am J Physiol Gastrointest Liver Physiol.* 1986;250:G391-G559.
- Strong AT, Landreneau JP, Cline M, et al. Per-oral pyloromyotomy (POP) for medically refractory post-surgical gastroparesis. *J Gastrointest Surg.* 2019;23:1095-1103.
- Mozwecz H, Pavel D, Pitrak D, Orellana P, Schlesinger PK, Layden TJ. Erythromycin stearate as prokinetic agent in post-vagotomy gastroparesis. *Dig Dis Sci.* 1990;35:902-905.
- Meng H, Zhou D, Jiang X, Ding W, Lu L. Incidence and risk factors for postsurgical gastroparesis syndrome after laparoscopic and open radical gastrectomy. *World J Surg Oncol.* 2013;11:1-5.
- Itoh Z, Suzuki T, Nakaya M, Inoue M, Mitsuhashi S. Gastrointestinal motor-stimulating activity of macrolide antibiotics and analysis of their side effects on the canine gut. *Antimicrob Agents Chemother.* 1984;26:863-869.
- Catnach SM, Fairclough PD. Erythromycin and the gut. *Gut.* 1992;33:397-401.

35. Deloose E, Verbeure W, Depoortere I, Tack J. Motilin: from gastric motility stimulation to hunger signalling. *Nat Rev Endocrinol.* 2019;15:238-250.
36. Mathis C, Malbert CH. Erythromycin gastrokinetic activity is partially vagally mediated. *Am J Physiol Gastrointest Liver Physiol.* 1998;1:G80-G86.
37. Parkman HP, Pagano AP, Vozzelli MA, Ryan JP. Gastrokinetic effects of erythromycin: myogenic and neurogenic mechanisms of action in rabbit stomach. *Am J Phys.* 1995;269:G418-G426.
38. Parkman HP, Pagano AP, Ryan JP. Erythromycin inhibits rabbit pyloric smooth muscle through neuronal motilin receptors. *Gastroenterology.* 1996;111:682-690.
39. Peeters TL. Erythromycin and other macrolides as prokinetic agents. *Gastroenterology.* 1993;105:1886-1899.
40. Janssens J, Peeters TL, Vantrappen G, et al. Improvement of gastric emptying in diabetic gastroparesis by erythromycin. *N Engl J Med.* 1990;322:1028-1031.
41. Sun WM, Smout A, Malbert C, et al. Relationship between surface electrogastrigraphy and antropyloric pressures. *Am J Physiol Gastrointest Liver Physiol.* 1995;268:G424-G430.
42. Bass P, Wiley JN. Electrical and extraluminal contractile force activity of the duodenum of the dog. *Am J Dig Dis.* 1965;10:183-200.
43. Wang TH-H, Du P, Angeli TR, et al. Relationships between gastric slow wave frequency, velocity, and extracellular amplitude studied by a joint experimental-theoretical approach. *Neurogastroenterol Motil.* 2018;30:e13152.
44. Hocke M, Schöne U, Richert H, et al. Every slow-wave impulse is associated with motor activity of the human stomach. *Am J Physiol Gastrointest Liver Physiol.* 2009;296:709-716.
45. Kuruppu S, Cheng LK, Avci R, Angeli-Gordon TR, Paskaranandavadivel N. Relationship between intestinal slow-waves, spike-bursts, and motility, as defined through high-resolution electrical and video mapping. *J Neurogastroenterol Motil.* 2022;28:664-677.
46. Carlson HC, Code CF, Nelson RA. Motor action of the canine gastroduodenal junction: a cineradiographic, pressure, and electric study. *Am J Dig Dis.* 1966;2:155-172.
47. Wang XY, Lammers WJEP, Bercik P, Huizinga JD. Lack of pyloric interstitial cells of Cajal explains distinct peristaltic motor patterns in stomach and small intestine. *Am J Physiol Gastrointest Liver Physiol.* 2005;289:G539-G549.
48. Somarajan S, Muszynski ND, Hawrami D, Olson JD, Cheng LK, Bradshaw LA. Noninvasive magnetogastrography detects erythromycin-induced effects on the gastric slow wave. *IEEE Trans Biomed Eng.* 2019;66:327-334.
49. Chen J, Yeaton P, McCallum RW. Effect of erythromycin on gastric myoelectrical activity in normal human subjects. *Am J Physiol Gastrointest Liver Physiol.* 1992;263:G24-G28.
50. Sanger GJ, Furness JB. Ghrelin and motilin receptors as drug targets for gastrointestinal disorders. *Nat Rev Gastroenterol Hepatol.* 2016;13:38-48.
51. Wang TH-H, Tokhi A, et al. Non-invasive thoracoabdominal mapping of postoesophagectomy conduit function. *BJS Open.* 2023;7(3):zrad036.
52. You CH, Chey WY, Lee KY, Menguy R, Bortoff A. Gastric and small intestinal myoelectric dysrhythmia associated with chronic intractable nausea and vomiting. *Ann Intern Med.* 1981;95:449-451.
53. Angeli TR, Cheng LK, Du P, et al. Loss of interstitial cells of Cajal and patterns of gastric dysrhythmia in patients with chronic unexplained nausea and vomiting. *Gastroenterology.* 2015;149:55-66.
54. Varghese C, Schamberg G, Calder S, et al. Normative values for body surface gastric mapping evaluations of gastric motility using gastric Alimetry: spectral analysis. *Am J Gastroenterol.* 2023;118:1047-1057.
55. Ali MK, Liu L, Chen JH, Huizinga JD. Optimizing autonomic function analysis via heart rate variability associated with motor activity of the human colon. *Front Physiol.* 2021;12:619722.
56. Wang TH-H, Angeli TR, et al. The influence of interstitial cells of Cajal loss and aging on slow wave conduction velocity in the human stomach. *Physiol Rep.* 2021;8(24):e14659.
57. Forster J, Damjanov I, Lin Z, Sarosiek I, Wetzel P, RW MC. Absence of the interstitial cells of Cajal in patients with gastroparesis and correlation with clinical findings. *Gastrointest Surg.* 2005;9:102-108.
58. Linke R, Meier M, Muenzing W, Folwaczny C, Schnell O, Tatsch K. Prokinetic therapy: what can be measured by gastric scintigraphy? *Nucl Med Commun.* 2005;26:527-533.
59. Aghababae Z, Wang TH-H, Nisbet LA, et al. Anaesthesia by intravenous propofol reduces the incidence of intra-operative gastric electrical slow-wave dysrhythmias compared to isoflurane. *Sci Rep.* 2023;13:11824.
60. Vazquez JAA, Bergstrom M, Bligh S, McMahon BP, Park P. Exploring pyloric dynamics in stenting using a distensibility technique. *Neurogastroenterol Motil.* 2018;30:1-8.
61. Tomomasa T, Kuroume T, Arai H, Wakabayashi K, Itoh Z. Erythromycin induces migrating motor complex in human gastrointestinal tract. *Dig Dis Sci.* 1986;31:157-161.
62. Yassi R, O'Grady G, Paskaranandavadivel N, et al. The gastrointestinal electrical mapping suite (GEMS): software for analyzing and visualizing high-resolution (multi-electrode) recordings in spatiotemporal detail. *BMC Gastroenterol.* 2012;12:60.

How to cite this article: Simmonds S, Wang T-H, Matthee A, et al. Pharmaceutical prokinetic and surgical interventions have opposing effects on gastroduodenal electromechanical coupling. *Acta Physiol.* 2025;241:e70024. doi:[10.1111/apha.70024](https://doi.org/10.1111/apha.70024)